Passive Detection of Image Splicing using Conditional Co-occurrence Probability Matrix

Xudong Zhao, Shilin Wang, Shenghong Li and Jianhua Li
Shanghai Jiao Tong University, Shanghai
E-mail: {zxd_1220, wsl, shli, lijh888}@sjtu.edu.cn Tel: +86-021-34205281

***Abstract*—In the past few years second order statistical features (e.g. Markov transition probability matrix) have been proved to be effective features for image forgery detection. In this paper, conditional co-occurrence probability matrix (CCPM) which is third order statistical features is proposed to detect image splicing. Since the dimensionality depends exponentially on the order of features, principal component analysis is employed to overcome the high dimensionality introduced computational complexity and over-fitting for a kernel based supervised classifier. Experimental results show that conditional co-occurrence probability matrix demonstrates its effectiveness in block discrete cosine transform domain, it outperforms Markov features in both block discrete cosine transform domain and spatial domain, principal component analysis is proved to be an effective dimensionality reduction method for image splicing detection.**

I. Introduction

Photograph forgery could be dated to 1860s [1], in the film camera era, only skilled forger with professional equipments could manipulate a film photograph, thus tampered photos are unfamiliar to many people. Nowadays we are living in a digital age, with the help of powerful digital image editing software and high performance computers, image forgeries flushed in our daily life. 'Seeing is Believing' is not applicable to digital images. In July 2008, an image of Iranian missile test which is shown in the left side of Fig. 1 appeared on the front pages of many newspapers. Shortly after its publication, it was proved to be a fake which was used to conceal a failing missile launch, and the original image is given in the right side of Fig. 1. In July 2010, British Petroleum (BP) struggling against the Gulf of Mexico oil spill posted a photo of its command center shown as left side of Fig. 2 on its website. Later, it was revealed that three screen images in the original photo were copied and pasted over three blank screens, and the manipulated photo was finally removed and replaced with the original photo shown in the right side of Fig. 2.

Fig. 1. Iranian missile test event.

Researchers have made efforts on digital image forensics, on the whole, all the detection methods can be reduced to active [2][3][4] and passive approaches [5]. Digital watermarking and signature have been proposed as active detecting methods, and they can be used to authenticate an image. However, the watermark or signature must be inserted at the time of imaging process which limit it to special equipped cameras, and many consumers' digital cameras do not have this function. On the contrary, passive detecting methods do not need any prior knowledge (e.g. watermark or signature), they work on the assumption that tampering will disturb the original underlying statistics of the image. For the above reasons, passive image detection gains much attention and it is becoming a hot research topic. This paper concerns the passive image forgery detection.

Fig. 2. Gulf of Mexico oil spill.

Several passive image detection methods have been proposed. Tian-Tsong Ng et al. in [6] proposed bicoherence which is a normalized bispectrum based features for image splicing detection. The best detecting performance over image data set [7] is 71%. W. Chen et al. in [8] proposed phase congruency and statistical moments of characteristic functions of wavelet sub-bands to catch the splicing artifacts. Experimental results showed that the best detecting accuracy over [7] is 82.3%. A natural image model consisting of statistical features was proposed in [9]. The statistical features were comprised of moments of characteristic functions of wavelet sub-bands and first order Markov transition probabilities of difference 2 D arrays. Detecting accuracies over [7] showed that 168 D moment features achieved 86.8% and 98 D first order Markov features achieved 88.3%. In [10], SIFT features were proposed to detect region duplications. SIFT features extracted from different regions were compared and correlations were employed to output a map indicating region with high probability to be duplicated from another one. When composing an image it is difficult for the forger to match the lighting conditions from the individual ones. Lighting inconsistencies can therefore be used to reveal the image tampering [11][12]. However, the proposed method failed in detecting the compositing part with the same lighting conditions. Color filter array (CFA) interpolations are employed to get a true color image for single CCD cameras. Correlations introduced by CFA interpolation are likely to be disturbed when tampering an image. For this reason, Popescu et al. in [13] proposed an interpolation based method to detect image forgeries, but this method failed in detecting low quality (high compressed rate) images. In [14] and [15], gray level co-occurrence matrix (GLCM) features and Run-length Run-number (RLRN) features extracted from Chroma spaces were employed to detecting image splicing, and experimental results showed that features extracted from Chroma spaces demonstrate much better class separability than that extracted from luma space. Both GLCM and RLRN features, however, do not get satisfying detecting performance over image data set [7].

Image splicing introduces sharp edges in a tampered image, thus capturing the tampering introduced artifacts is the key for image splicing detection. Since edges introduced by tampering are different with their "neighbors", the relationships between spliced parts and normal parts can be used to expose image forgery. In this paper, relationships between elements in an array are modeled as conditional co-occurrence probability matrix (CCPM) which contains more informative features compared with first order (e.g. histogram) and second order (e.g. Markov features) statistics. We test the proposed method in block discrete cosine transform (BDCT) domain and spatial domain, and the conditional co-occurrence probability matrix demonstrates its superiority in BDCT domain compared with spatial domain. CCPM (third order statistical features) contains discriminative information, however the dimensionality of features exponentially increases with the order. For a large number of modern machine learning algorithms, high dimensionality usually introduces computational complexity and over-fitting [16]. Therefore, principal component analysis (PCA) is introduced in our work to reduce the dimensionality of proposed features. Experimental results show that CCPM superior to Markov features in both BDCT and spatial domains, PCA can reduce the dimensionality of proposed features greatly without bringing down classification performance.

The rest of this paper is organized as follow. The proposed method is described in section II. In section III, the experimental work and detecting performance analysis are reported. Finally, conclusions and future works are given in section IV.

II. PROPOSED METHOD

A. Preprocessing

One purpose of image splicing detection is to get the features independent of image contents. Since, features which are dependent on image contents usually lead to poor generalization ability. In our work, image is de-correlated [9] before extracting features, that is, subtraction between neighboring elements which can be formulated as:

$$E_h(i,j) = I(i,j) - I(i+1,j) \tag{1}$$

$$E_v(i,j) = I(i,j) - I(i,j+1), \tag{2}$$

where $I(i,j)$ is the value of image pixel intensity or DCT coefficient at the position (i,j), $E_h(i,j)$ and $E_v(i,j)$ indicate de-correlated arrays along horizontal right and vertical down directions respectively. In this paper we investigate the effectiveness of CCPM in both spatial domain and BDCT domain. For spatial method, I denotes the input image, $E_h(i,j)$ and $E_v(i,j)$ are the edge images along horizontal and vertical direction, an example is given in Fig. 3. Two horizontally spliced images and two vertically spliced images are shown in the first row. $E_h(i,j)$ and $E_v(i,j)$ of the spliced images are given in the second row and the third row. From the figure we can see that horizontally spliced parts are emphasized in the horizontally de-correlated images, and vertically de-correlated images put emphasis on the vertically spliced parts.

For DCT method, I is the 8×8 non-overlapping BDCT of the input image which is given as

$$I = \begin{pmatrix} I_{11} & I_{12} & \cdots & I_{1m} \\ I_{21} & I_{22} & \cdots & I_{2m} \\ \vdots & \vdots & \cdots & \vdots \\ I_{m1} & I_{m2} & \cdots & I_{mm} \end{pmatrix}, \tag{3}$$

where $I_{ij} (1 \le i,j \le m)$ is a 8×8 block DCT coefficients array, m is the number of 8×8 blocks in a row or column. I_{ij} is defined as

$$I_{ij} = U^T I^s_{ij} U, \tag{4}$$

where I^s_{ij} is the corresponding 8×8 image block and U is given by

$$\begin{cases} U(n,k) = \frac{1}{2\sqrt{2}}, & k = 0, 0 \le n \le 7 \\ U(n,k) = \frac{1}{2}\cos(\frac{\pi(2n+1)k}{16}), & 1 \le k \le 7, 0 \le n \le 7 \end{cases} \tag{5}$$

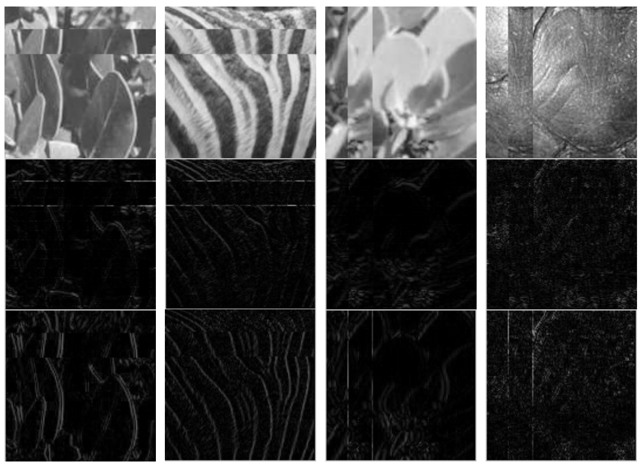

Fig. 3. Spliced images and the corresponding de-correlated images. Spliced images are showed in the first row; horizontally de-correlated images and vertically de-correlated images are given in the last two rows.

B. CCPM Modeling

Markov chain is commonly used to describe the underlying class dependences. For classes $\omega_1, \omega_2, \cdots, \omega_N$ (N is the total number of classes), Markov model assumes that

$$P(\omega_{i_k}|\omega_{i_{k-1}}, \omega_{i_{k-2}}, \cdots, \omega_{i_1}) = P(\omega_{i_k}|\omega_{i_{k-1}}). \quad (6)$$

The meaning of (6) is that class dependence is limited only within two successive classes (i.e. second order statistics). In our work, we expand the Markov model to CCPM model which defined as

$$P(\omega_{i_k}, \omega_{i_{k-1}}|\omega_{i_{k-2}}). \quad (7)$$

That is, we consider the class dependence within three successive classes (i.e. third order statistics). CCPM with size $N \times N^2$ is given as

$$CCPM = \begin{bmatrix} p_{111} & p_{121} & \cdots & p_{1NN} \\ p_{211} & p_{221} & \cdots & p_{2NN} \\ \vdots & \vdots & \cdots & \vdots \\ p_{N11} & p_{N21} & \cdots & p_{NNN} \end{bmatrix}, \quad (8)$$

where $p_{abc} \equiv P(\omega_c, \omega_b|\omega_a)$ $(1 \leq a, b, c \leq N)$ is the co-occurrence probability of the next two classes (ω_c, ω_b) if the current class is ω_a, and $\sum_{b,c=1}^{N} p_{abc} = 1$. Every element in an 2 D array has 8 neighbors (boundary elements are neglected), therefore there exists 8 directional CCPMs to describe the dependences between different classes. For computational convenience, we use horizontal right and vertical down directional CCPMs which are denoted as CCPM$_h$ and CCPM$_v$ as features for classification, thus, the dimensionality of features is $2N^3$. The selection of N greatly influence the dimensionality of proposed features, in our work, we threshold CCPM$_h$ and CCPM$_v$ in the range [-3, 3], that is, totally 7 classes are considered in our work. Fig. 4 illustrates the feature extraction process in the spatial domain and BDCT domain.

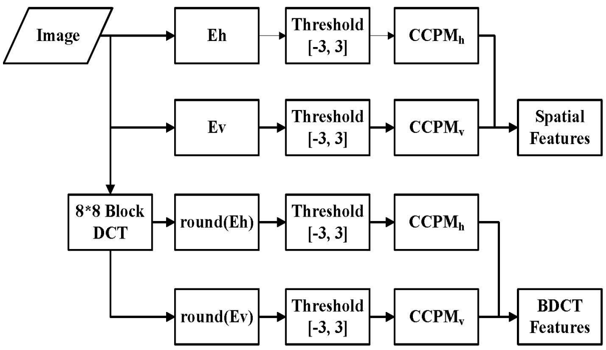

Fig. 4. CCPM feature extraction in spatial domain and BDCT domain.

C. Dimensionality Reduction for Features

A problem associated with CCPM features is the high dimensionality. Obviously, high dimensionality will introduce computational complexity. Furthermore, although single feature carries discriminative information respectively, when combined together there is little gain if they are highly correlated. Curse of dimensionality is also an import reason for dimensionality reduction.

There exist high correlations between CCPM features, thus PCA is introduced in our work to avoid information redundancies. Let

$$Y = A^T(X - \bar{X}), \quad (9)$$

where X is original feature vector matrix with D rows (feature dimensionality) and K columns (number of samples), Y is the new feature vector matrix with d rows (dimensionality of transformed features) and K columns,$\bar{X}$ denotes the mean value of X. Correlation matrix R_y is defined as

$$R_y \equiv E(YY^T) = A^T cov_{X-\bar{X}} A, \quad (10)$$

$cov_{X-\bar{X}}$ is the covariance matrix of $X - \bar{X}$ and it is symmetric, hence its eigenvectors are mutually orthogonal. When A is comprised of eigenvectors of $cov_{X-\bar{X}}$, R_y is then a diagonal matrix, i.e. features in Y are uncorrelated. Therefore A can be formulated as $[v_1, v_2, \cdots, v_D]$, v_i $(i = 1, 2, \cdots, D)$ is the eigenvector corresponding to eigenvalue λ_i of $cov_{X-\bar{X}}$ and $\lambda_1 > \lambda_2 > \cdots > \lambda_D$ which makes $var(v_1) > var(v_2) > \cdots > var(v_D)$. Y is therefore the projection of X onto the subspace spanned by the eigenvectors and the significance of features decreases with the increasing of dimensionality. Fig. 5 indicates the relationship between the dimensionality and variance of the corresponding features of Markov and CCPM after PCA dimensionality reduction. It can be seen from the figure that variances of features drops dramatically with the increase of dimensionality, i.e. the first d $(d < D)$ features take most information of Y and they can be used to represent Y. d is selected in our work according to the detection accuracy.

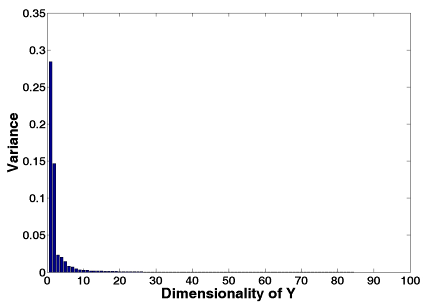

(a)

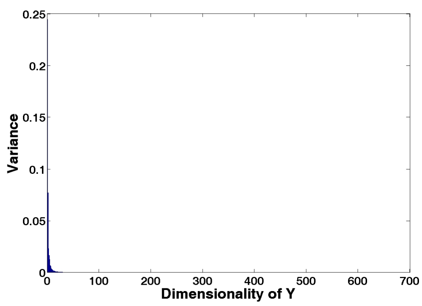

(b)

Fig. 5. Variance distribution of Y. (a) Markov, (b) CCPM.

III. EXPERIMENTAL RESULTS AND PERFORMANCE ANALYSIS

A. Image Dataset

To test the effectiveness of the proposed method, Columbia Image Splicing Detection Evaluation Dataset [7] which consists of 933 authentic and 912 spliced images is used in our experimental work. The image dataset covers a variety of images (e.g. smooth, textured, arbitrary object boundary and straight boundary). Images in this dataset are all in BMP format with fixed size of 128×128. Spliced images are manipulated via two types of operations, that is, crop and past of horizontal or vertical strips and crop and past along object boundaries. The spliced parts can be from the same image or from another image. Some of the images are given in Fig. 6.

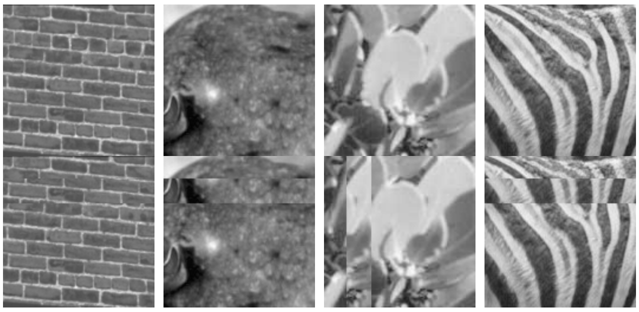

Fig. 6. Some image examples in image set [7]. Authentic images are shown in the first row and spliced ones are given in the second row.

B. Classifier

Support vector machine (SVM) which is a supervised machine learning method is employed in our work for classification. LIBSVM [17] is used as classifier and radial basis function (RBF) is selected as kernel of SVM. For each experiment, half of the authentic images and half of the spliced images are randomly selected to train the SVM, and the left authentic and spliced images are treated as test set. Grid searching is employed to select the best parameters C (positive constant that controls the relative influence of the competing terms) and γ (variance of RBF kernel) for SVM. This procedure is repeated thirty times to eliminate the effect of randomness. Experimental results are evaluated by the average detecting accuracies over thirty times and receiver operating characteristics curves (ROC).

C. Comparisons

Experimental results of proposed CCPM features with dimensionality 686 and Markov features [9] with dimensionality 98 are given in Table I, where TP, TN and Accuracy denote true positive rate, true negative rate and the average detection rate over thirty runs respectively. Standard deviations over thirty random tests are given in the parentheses. Table I shows that the proposed CCPM features outperform first order Markov features in both spatial domain and BDCT domain. Fig. 7 indicates detecting performance comparisons between Markov features and CCPM features after PCA dimensionality reduction. Note that the first 98 D PCA features of CCPM is employed for the convenience of comparison.

TABLE I
COMPARISONS OF DETECTION ACCURACIES BETWEEN MARKOV FEATURES AND CCPM FEATURES

	Spatial domain			BDCT domain		
	TP	TN	Accuracy	TP	TN	Accuracy
Markov	74.0% (2.612)	78.1% (2.307)	76.0% (1.116)	84.1% (1.907)	89.5% (1.854)	86.8% (0.719)
CCPM	78.5% (1.893)	75.7% (2.190)	77.1% (1.105)	85.7% (1.935)	91.3% (1.602)	88.5% (0.890)

From Fig. 7 we can see that:

(1) Markov and CCPM features demonstrate much better detecting performance in BDCT domain than that in spatial domain.

(2) Detection performance increases dramatically for the first few features, after that it vibrates on a small scale.

(3) CCPM outperforms Markov features in BDCT domain with PCA dimensionality more than 10.

(4) In spatial domain, CCPM outperforms Markov features when PCA dimensionality is larger than 45.

(5) Compared with Table I, features after PCA dimensionality reduction can perform as well as original features do, in some cases, even better than the original features.

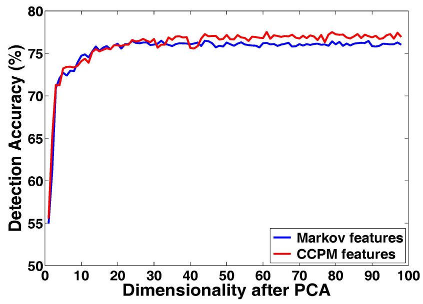

(a)

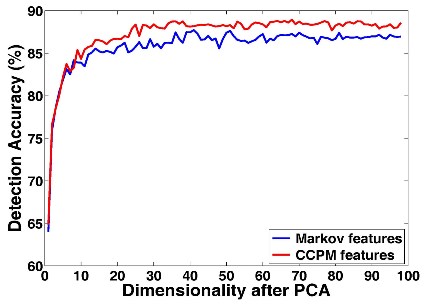

(b)

Fig. 7. Comparisons of detecting performance between Markov features and CCPM after PCA dimensionality reduction. (a) Spatial domain, (b) BDCT domain.

To testify the effectiveness of PCA for dimensionality reduction, boosting feature selection method proposed in [14] is employed in our work for comparison, and the comparison results are given in Fig. 8. It can be seen from Fig. 8 that the performance of PCA dimensionality reduction outperforms boosting feature selection dramatically in both BDCT domain and spatial domain.

Finally, we employ the first 30 D PCA features to compare with the original features in BDCT domain, and the receiver operating characteristics (ROC) curves are given in Fig. 9 (a). In a similar way, Fig. 9 (b) illustrates the comparison results between the first 45 D PCA features and the original feature in spatial domain. From Fig. 9 we can find that, CCPM features in BDCT domain can be reduced to as few as 30 D from the original 686 D without losing discriminative information, and the spatial CCPM features can be reduced to 45 D without discriminative information loss.

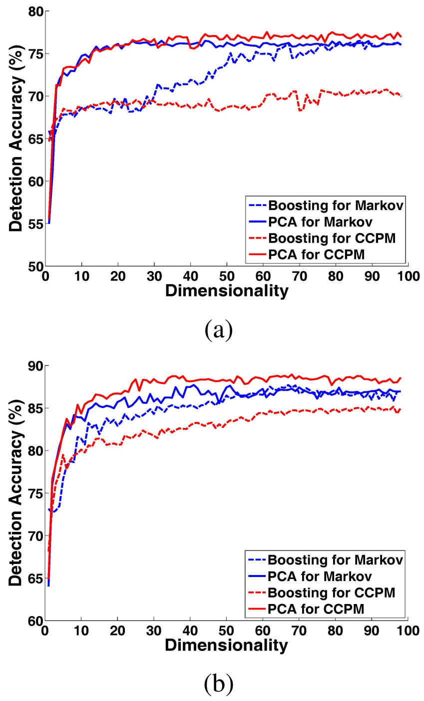

Fig. 8. Detection performance comparisons between PCA dimensionality reduction and boosting feature selection method for both Markov features and CCPM features. (a) Spatial domain, (b) BDCT domain.

IV. Conclusions

Passive image splicing detection is becoming a hot research topic. Different kinds of features have been proposed in the past few years, and Markov transition probability matrix is one of the most effective features. In this paper, CCPM is proposed for image splicing detection, that is, we consider the class dependences within three successive classes and the transition probability from the current class to the next two classes is treated as discriminative feature. All the conditional co-occurrence probabilities are grouped into CCPM and the matrix is then fed into SVM for classification. Higher order statistical features contain more discriminative information while the high dimensionality usually leads to computational complexity and over-fitting for modern supervised classifier. PCA is therefore proposed for dimensionality reduction. We test the effectiveness of CCPM in both BDCT domain and spatial domain. Experimental results have shown that CCPM demonstrates much better performance in BDCT domain than that in spatial domain, and in both domains CCPM outperforms Markov features. PCA is testified as an effective tool for image splicing detection, it can reduce the dimensionality of original features greatly without losing discriminative information. Higher order features integrated with dimensionality reduction method will be further studied in our future work.

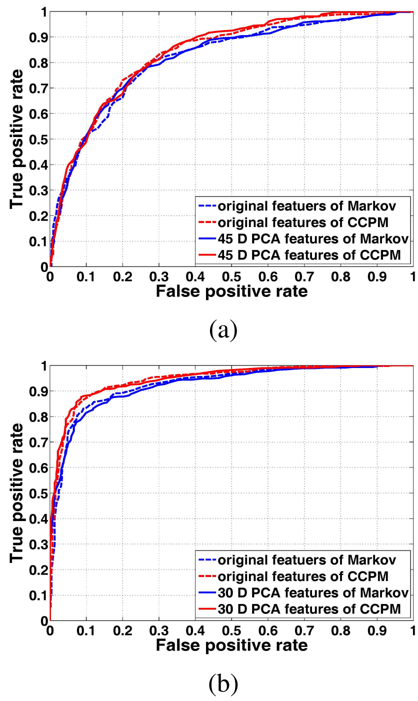

Fig. 9. Receiver operating characteristics curves. (a) 45 D PCA features and the original features in spatial domain, (b) 30 D PCA features and the original features in BDCT domain.

Acknowledgment

This research work is funded by the National Science Foundation of China (61071152, 60702043), 973 Program (2010CB731403, 2010CB731406) of China, Shanghai Educational Development Foundation and Beijing Key Laboratory Program of Communication and Information System of Beijing Jiaotong University. Credits for the use of the Columbia Image Splicing Detection Evaluation Dataset are given to the DVMM Laboratory of Columbia University, CalPhotos Digital Library and the photographers listed in http://www.ee.columbia.edu/ln/dvmm/downloads/AuthSplicedDataSet/photographers.htm.

References

[1] Photo tampering throughout history, http://www.cs.dartmouth.edu/farid/research/digitaltampering.

[2] S. Katzenbeisser and F. A. P. Petitcolas, "Information techniques for steganography and digital watermarking," *Norwood, MA: Artec House,* 2000.

[3] I. J. Cox, M. L. Miller, and J. A. Bloom, "Digital watermarking," *San Francisco, CA: Morgan Kaufmann,* 2002.

[4] C. Rey and J.L. Dugelay, "A survey of watermarking algorithms for image authentication," *EURASIP Journal on Applied Signal Processing,* vol. 2002 (6), pp. 613-621, March 2002.

[5] Hany Farid: "A survey of image forgery detection," *IEEE Signal Processing Magazine,* vol. 26 (2), pp. 16-25, 2009.

[6] Tian Tsong Ng, Shih-Fu Chang, and Qibin Sun, "Blind detection of photomontage using higher order statistics," *IEEE International Symposium on Circuits and Systems,* 2004.

[7] Columbia DVMM Research Lab. "Columbia Image Splicing Detection Evaluation Dataset," http://www.ee.columbia.edu/ln/dvmm/downloads/AuthSplicedDataSet/AuthSplicedDataSet.htm.

[8] W. Chen, Y.Q. Shi, and W. Su, "Image splicing detection using 2-d phase congruency and statistical moments of characteristic function," *in Society of Photo-Optical Instrumentation Engineers (SPIE) Conference Series,* vol. 6505, February 2007.

[9] Yun Q. Shi, Chunhua Chen and Wen Chen, "A natural image model approach to splicing detection," *ACM Proceedings of the 9th workshop on Multimedia & security,* 2007.

[10] Xunyu Pan and Siwei Lyu, "Detecting image region duplication using SIFT features," *Acoustics Speech and Signal Processing (ICASSP),* 2010.

[11] M.K. Johnson and H. Farid, "Exposing digital forgeries by detecting inconsistencies in lighting," *ACM Proceedings of the 7th Workshop on Multimedia and Security,* pp. 1-10, 2005.

[12] M.K. Johnson, H. Farid, "Exposing digital forgeries in complex lighting environments," *IEEE Transactions on Information Forensics and Security,* vol. 2 (3), pp. 450 - 461, 2007.

[13] Popescu A C and Farid H, "Exposing digital forgeries in color filter array interpolated images," *IEEE Transactions on Signal Processing,* vol. 53 (10), pp. 3948-3959 (2005)

[14] Wei Wang, Jing Dong and Tieniu Tan, "Effective image splicing detection based on image chroma," *International Conference on Image Processing (ICIP),* 2009.

[15] Xudong Zhao, Jianhua Li, Shenghong Li and Shilin Wang, "Detecting digital image splicing in chroma spaces," *International Workshop on Digital Watermarking,* 2010, *LNCS* vol. 6526, pp. 12-22, 2011.

[16] Y. Bengio, O. Delalleau and N. Le Roux, "The curse of dimensionality for local kernel machines," *Technical report TR 1258,* 2005.

[17] C.C. Chang and C.J. Lin, "LIBSVM: a library for support vector machines," 2001, http://www.csie.ntu.edu.tw/?cjlin/libsvm.